Journal of Applied Polymer Science

Preparation and characterization of high MFR polypropylene and polypropylene/poly(ethylene-*co*-propylene) in-reactor alloys

Biao Zhang,[1] Zhisheng Fu,[1] Zhiqiang Fan,[1] Phairat Phiriyawirut,[2] Sumate Charoenchaidet[2]
[1]Department of Polymer Science & Engineering, Zhejiang University, Hangzhou, 310017, China
[2]SCG Chemicals Co., Ltd., 1 Siam Cement Road, Bangkok, 10800, Thailand
Correspondence to: Z. Fu (E-mail: fuzs@zju.edu.cn)

ABSTRACT: In this work, high melt flow rate (MFR) polypropylene (HF-PP) and polypropylene/poly(ethylene-*co*-propylene) in-reactor alloys (HF-PP/EPR) with MFR ≈ 30 g/10 min were synthesized by spherical $MgCl_2$-supported Ziegler–Natta catalyst with cyclohexylmethyldimethoxysilane (CHMDMS) or dicyclopentyldimethoxysilane (DCPDMS) as external donor (De). The effects of De on polymerization activity, chain structure, mechanical properties, and phase morphology of HF-PP and HF-PP/EPR were studied. Adding CHMDMS caused more sensitive change of the polymers MFR with H_2 than DCPDMS, and produced PP/EPR alloys containing more random ethylene-propylene copolymer (r-EP) and segmented ethylene-propylene copolymer (s-EP). CHMDMS also caused formation of s-EP with higher level of blockiness than DCPDMS. HF-PP/EPR alloy prepared in the presence of DCPDMS exhibited higher flexural properties but lower impact strength than that prepared with CHMDMS. Toughening efficiency of the rubber phase was nearly the same in the alloys prepared using CHMDMS or DCPDMS as De, but stiffness of the alloy can be improved by using DCPDMS. © 2015 Wiley Periodicals, Inc. J. Appl. Polym. Sci. **2016**, *133*, 42984.

KEYWORDS: characterization; copolymers; polyolefins; properties

Received 12 June 2015; accepted 23 September 2015
DOI: 10.1002/app.42984

INTRODUCTION

Polypropylene (PP), as one of the most important general purpose plastics, has been extensively applied in various industries due to its excellent thermal and mechanical properties, chemical resistance, and processing features.[1–3] However, PP prepared with Ziegler–Natta catalysts under conventional conditions often has a high molecular weight ($M_w > 200 \times 10^3$) or low melt flow rate (MFR ≤ 5).[4–7] Such low MFR significantly limits its efficient processing in certain important applications like fiber spinning and injection molding of large-size automobile parts with intricate shape. As a result, high MFR polypropylene (HF-PP) resin is especially favored in the plastics market, for the high melt fluidity enables easy processing, and thus enhances production rate by shortening molding cycle. Besides, HF-PP can be made into thin wall products, reducing raw materials requirement.[8–12] Hydrogen is commonly used as an effective chain transfer agent to reduce the polymer molecular weight in olefin polymerization. This chain transfer agent can be effectively applied in olefin polymerization systems with different catalysts, cocatalysts, and electronic donors.[13–18] By changing the volume of hydrogen added to the polymerization system, MFR of PP can be effectively tailored in a broad range. Among the two main approaches of enhancing MFR of PP, namely controlled-rheology (CR) technique[19] and hydrogen addition during polymerization,[20] the latter is more preferable for simplicity of operation, as the CR technique exerts a secondary processing of the resin and thus consumes more energy. What is more important, HF-PP synthesized by adding hydrogen is more transparent and involves no volatile organic compounds.[10]

Just as common isotactic PP, the application of HF-PP is still limited by its high notch sensitivity and poor impact resistance, especially at low temperature and high strain rate,[21–25] and the limitation is even stronger for its lower molecular weight. To solve these problems, great efforts have been made to work out better modification methods. Recently, Jiang *et al.* investigated the effect of two nucleators, NA-21 and WBG, on crystallization and mechanical properties of HF-PP, finding that both can increase the crystallization rate, flexural strength, and impact strength of the resin. However, NA-21 improves the stiffness efficiently, while the latter is beneficial to improvement of

Additional Supporting Information may be found in the online version of this article.

toughness.[10] Later, they reported the properties of blends of HF-PP/metallocene poly(ethylene–butene–hexene) copolymer (HF-PP/mEBHC) prepared by melt-blending. It showed that toughness of the blends increased significantly with the content of mEBHC both at 23°C and −20°C.[11] As a more efficient and economical way of toughening PP resins, in-reactor blending of PP with other polyolefins (e.g., ethylene–propylene copolymer, EPR) by sequential multistage polymerization has been intensively studied in the last two decades.[4,5,26–38] However, synthesis and structure of PP/EPR in-reactor blends or in-reactor alloys with MFR ≥ 25 g/10 min (HF-PP/EPR) have not been reported in literatures up to now. For its excellent mechanical properties and good processability, this kind of materials finds broad applications in automobile and electric appliances industry, and is highly demanded in the plastics market.

Comparing with PP and PP/EPR in-reactor alloys of medium-to-low MFR, production of HF-PP and HF-PP/EPR meet extra difficulties caused by the severe changes of polymer chain structure with the hydrogen concentration. Zohuri *et al.* reported that hydrogen caused evident decrease of PP's isotacticity index in propylene polymerization with $MgCl_2$-supported Ziegler–Natta catalysts.[39] Soares *et al.* found that the microisotacticity ([mmmm]) of PP was enhanced by increasing the amount of hydrogen.[40] It was also reported by van Reenen *et al.* that the effect of hydrogen on the tacticity of PP greatly depended on whether an external donor was introduced in the polymerization.[41] In a previous work, we found that the ethylene content of ethylene–propylene copolymer synthesized with $MgCl_2$-supported Ziegler–Natta catalysts was lowered by small amount of hydrogen.[42] These changes in the chain structure of PP and EPR will inevitably influence the properties of HF-PP and HF-PP/EPR alloys. For this reason, it is necessary to study the structure and properties of HF-PP and HF-PP/EPR alloys and search for better ways to optimize the performances of the resins.

Alkoxysilanes are widely used as external donor (De) in propylene polymerization with $MgCl_2$-supported Ziegler–Natta catalysts for enhancing isotacticity of the polymer.[6,43–51] Among various $R_1R_2Si(OMe)_2$ type De, dicyclopentyldimethoxysilane (DCPDMS) showed especially strong ability to enhance PP's isotacticity without sacrificing the catalyst activity.[40,43,47,50] However, the sensitivity of polymer's molecular weight to hydrogen concentration becomes worse when DCPDMS was used as De. In other words, comparing to the more frequently used De like cyclohexylmethyldimethoxysilane (CHMDMS), more hydrogen is needed to increase MFR of polymer to the same level when DCPDMS is used as De. It is still unclear how the steric bulkiness of alkyl groups in $R_1R_2Si(OMe)_2$ type De will influence the structure and properties of PP and PP/EPR in-reactor alloys synthesized in the presence of relatively large amount of hydrogen.

In this work, HF-PP and HF-PP/EPR with MFR ≈ 30 g/10 min were, respectively, synthesized with a commercial $MgCl_2$-supported Ziegler–Natta catalyst in the presence of CHMDMS or DCPDMS. Chain structure, thermal behaviors, mechanical properties of the HF-PP and HF-PP/EPR alloys, as well as phase morphology of the HF-PP/EPR alloys were studied.

EXPERIMENTAL

Materials

A commercial $MgCl_2$-supported Ziegler–Natta catalyst ($MgCl_2$/dibutylphalate/$TiCl_4$, obtained from SINOPEC, China) with spherical particle shape and Ti content of 2.65 wt % was used for polymerization. Ethylene and propylene (polymerization grade, product of SINOPEC Shanghai Petrochemical Co., Ltd.) were further purified by passing through a column packed with deoxygen reagent and molecular sieves. Hydrogen (>99.999%) was further purified by passing through a column packed with molecular sieves. $Al(C_2H_5)_3$ (TEA) was purchased from Albemarle Co. and diluted in *n*-heptane to 2 mol/L before use. Cyclohexylmethyldimethoxysilane (CHMDMS) and dicyclopentyldimethoxysilane (DCPDMS) were supplied by Linyi Lujing Chemical Co. (Shandong, China) and distilled before use.

Synthesis of PP/EPR In-Reactor Alloy

The apparatus for synthesizing HF-PP and HF-PP/EPR in-reactor alloys has been described in our previous work.[33] The polymerization procedure was composed of three steps: prepolymerization of propylene in slurry, homopolymerization of propylene in slurry, and ethylene–propylene copolymerization in gas phase. In the prepolymerization stage, slurry polymerization of propylene was conducted in a 0.8 L stainless steel jacketed autoclave for 15 min. About 50 mg catalyst was used in the polymerization. Triethylaluminum ($AlEt_3$) at Al/Ti = 100 as cocatalyst was added to 100 mL *n*-heptane, then CHMDMS or DCPDMS at Si/Ti = 5 was added. The solution was then saturated with propylene at 0.1 MPa and 30°C. Under mechanical stirring of about 300 rpm, the catalyst was added to the autoclave to start the prepolymerization. After 15 min, designated amount of H_2 was injected to the autoclave, then propylene at 0.6 MPa was introduced to the autoclave, and the temperature was raised to 75°C. Propylene homopolymerization was then carried out for 2 h. During this period, the stirring speed was adjusted to 100 rpm After 10 min reaction, propylene and solvent in the autoclave were removed by evacuation to 5 mmHg for 10 min, and then gas phase copolymerization of ethylene and propylene was started by continuously supplying ethylene/propylene/H_2 mixture at 0.3 MPa to the autoclave through an inlet pipe at the bottom of the autoclave (see ref. 4). The gaseous mixture of ethylene, propylene, and hydrogen in molar ratio of 1:1.2:0.022 (ethylene:propylene:H_2) has been prepared and stored in a gas tank before the polymerization experiment. During the copolymerization, the monomer mixture was simultaneously discharged from a vent-pipe on the cover of the autoclave to keep a nearly constant monomer composition in the autoclave. After running the copolymerization for 25 min at 75°C, it was terminated by stopping the monomer flow, venting the autoclave, and pouring the polymer particles into excess of ethanol containing 5% HCl. The solid product was recovered by filtering and washed with ethanol for three times. Subsequently, the copolymer was dried in vacuum at 60°C for 12 h.

Homopolymerization of HF-PP

Propylene homopolymerization was conducted using the same apparatus in a two-stage process. The conditions and operations

are the same as the prepolymerization and homopolymerization stages in synthesizing the HF-PP/EPR alloys.

Fractionation of HF-PP and HF-PP/EPR In-Reactor Alloy

Procedures of fractionation of the HF-PP/EPR samples by successive solvent extractions are the same as mentioned in the previous work.[4] Each alloy sample was fractionated into three parts: *n*-octane soluble part (C8-sol), boiling *n*-heptane soluble part (C7-sol), and boiling *n*-heptane insoluble part (C7-insol). The same procedures were adopted to fractionate the PP samples into three parts.

Determination of MFR

As specified in GB/T 3682-2000, the MFR of each sample was determined by using a melt flow index tester (ZRZ1452, MTS Systems (China) Co., Ltd) at 230°C ± 0.5°C under a 2.16 kg load. The diameter of the die is 2.095 ± 0.005 mm. Every 5 seconds there was a cutting, and then at least five cutting specimens without bubble were selected. The MFR is defined as the extrudate weight in grams per 10 min and can be calculated as follows:

$$\mathrm{MFR} = t_{\mathrm{ref}} \cdot m/t \quad (1)$$

where t_{ref}, reference time (10 min); m, average weight of cutting specimen; and t, cutting interval (5 s).

Measurement of Molecular Weight

The molecular weights and molecular weight distributions of the fractions were measured by gel permeation chromatography (GPC) in a PL 220 GPC instrument (Polymer Laboratories, Ltd.) at 150°C in 1,2,4-trichlorobenzene with 0.0125% antioxidant BHT. Three PL mixed B columns (500 ~ 10^7) were used. Universal calibration against narrow polystyrene standards was adopted.

Nuclear Magnetic Resonance Analysis

^{13}C NMR spectra of the polymer fractions were recorded on a Varian Mercury 300-plus spectrometer at 75 MHz. *o*-Dichlorobenzene-d_4 was used as the solvent, and the sample concentration was 10 w/v %. The spectra were recorded at 120°C with hexamethyldisiloxane as an internal chemical shift reference. $Cr(acac)_3$ was used to reduce the relaxation time of carbon atoms, and the delay time was set as 3 s. The pulse angle was 90° and more than 4000 transients were collected.

Thermal Analysis

Differential scanning calorimetry (DSC) analysis was measured on a TA Q200 thermal analyzer under a high purity nitrogen atmosphere. About 5 mg of the sample was sealed in an aluminum pan. The sample was first heated to 180°C and kept for 5 min in order to erase the previous thermal history, and then cooled down to 40°C at a rate of 10°C/min. Finally, it was heated up to 180°C at the rate of 10°C/min again, and heat flow in the second heating scan was recorded.

Measurement of Mechanical Properties

Polymer granules were melted and mixed by a HAAKE torque rheometer at 180°C for 8 min, and then compressed-molded to specimens of 80 × 10 × 4 mm on a platen press at 180°C under 17.5 MPa. According to ISO 179 and ISO 180, the notched Charpy impact strength and Izod impact strength were measured. The flexural modulus was measured on an electronic tester following ISO 178. For each sample, five parallel specimens were tested and the average value was adopted.

Table I. Polymerization Behaviors of HF-PP and HF-PP/EPR Alloys

Samples	De	H_2 (mol %)	Activity (kg/g cat · h)	MFR (g/10 min)
PP-1	CHMDMS	1.9	1.10	31.2
PP-2	DCPDMS	3.8	1.34	30.2
Alloy-1	CHMDMS	2.2	1.18	29.5
Alloy-2	DCPDMS	4.5	1.09	32.1

Scanning Electron Microscopy (SEM)

Phase morphology and dispersion state of EPR domains in the PP matrix were investigated by a Hitachi s-4800 field emission scanning electron microscope. The SEM samples were prepared as follows: Specimens prepared as described above were fractured in liquid nitrogen and etched by xylene under ultrasonic at 50°C for 5 min. After 24 h, the etched surfaces were sputtered with platinum and finally subjected to SEM observation. The morphology of impact fractured surfaces was also observed in SEM after sputtered with platinum.

RESULTS AND DISCUSSION

Polymerization Behaviors

In order to regulate the MFR of PP and PP/EPR in-reactor alloy to the designed value (about 30 g/10 min), a series of polymerization experiments with different H_2/monomer ratios in the propylene polymerization stage were conducted. Table I lists the results of synthesizing PP and PP/EPR in-reactor alloy under the optimized conditions. By adding suitable amount of hydrogen, MFR of the PP and PP/EPR samples were all around 30 g/10 min. Comparing with the PP samples, a little more H_2 was needed to regulate MFR of the alloys to about 30. Among the two external donors, much more H_2 was needed when D-donor was used, meaning that C-donor is more sensitive to H_2. Similar phenomena have been reported in literatures.[40,43]

Results of Fractionation and GPC Analysis

Because different types of active centers are present in supported Ziegler–Natta catalysts, polypropylene and its copolymer with ethylene are actually composed of polymer chains of evidently different chain characteristics, for example, different stereoregularity, comonomer content, comonomer sequence distribution, and molecular weight.[26,43,47] In order to determine the polymer composition and make a better understanding of the relations between polymer chain structure and properties, each of the four samples in Table I was fractionated by two-step solvent extractions into three parts, namely C8-sol, C7-sol, and C7-insol. The amount of the fractions is summarized in Table II. For the PP samples, the C8-sol fraction is almost pure atactic PP chains.[47] It was shown in Table II that adding DCPDMS can reduce the amount of atactic PP more efficiently than CHMDMS in the homopolymerization stage. This trend is the same as observed in propylene polymerization in the absence of hydrogen.[47] A generally accepted mechanism is that alkoxysilane

Table II. Fractionation Results (wt %) and Molecular Weight (kg/mol) of each Fraction in HF-PP and HF-PP/EPR Alloys

				M_w (C8-sol)		M_w (C7-sol)		
Entry	C8-sol	C7-sol	C7-insol	Peak 1[a]	Peak 2[b]	Peak 1[a]	Peak 2[b]	M_w (C7-insol)
PP-1	1.5	3.4	95.1	1.0	60.0	17.2		193
PP-2	0.9	3.8	95.3	1.1	53.1	12.9		187
Alloy-1	17.2	7.0	75.8	0.9(1.2)[c]	151(98.8)	5.4(33.6)	139(66.4)	175
Alloy-2	12.9	5.8	81.3	0.9(1.5)	176(98.5)	6.0(47.2)	208(52.8)	171

[a] The peak with lower molecular weight in the bimodal MWD curve.
[b] The peak with higher molecular weight in the bimodal MWD curve.
[c] Data in the parentheses are weight percentage of the peak in the MWD curve.

can complex with both the active sites and the cocatalyst. Bulky substituents on alkoxysilane are required to prevent the De from leaving the catalyst surface through complexation with the cocatalyst. Bearing two bulky cyclopentyl groups, DCPDMS can thus cause larger extent of isotacticity improvement than CHMDMS. However, increase in the percentage of isotactic PP (C7-insol) by using DCPDMS appeared extremely small, which was in contrast to the phenomena observed in our previous works.[47,52] This could be ascribed to increase in the amount of low molecular weight isotactic PP chains that soluble in cold *n*-octane or boiling *n*-heptane. Comparing to CHMDMS, twice amount of H_2 was employed in synthesizing PP using DCPDMS as external donor, so more isotactic PP chains would be extracted into C8-sol and C7-sol fractions. In synthesizing the alloys, contents of both C8-sol and C7-sol fractions in alloy-1 were higher than that in alloy-2. Because the C8-sol and C7-sol fractions are mainly composed of copolymer chains,[27] this difference means that using DCPDMS would reduce the copolymerization activity.

Molecular weight distributions (MWD) of the fractions were measured by GPC. Figure 1 shows the MWD curves of the two C8-sol fractions from PP-1 and PP-2, respectively. Bimodal distribution of this PP fraction means that it is composed of two kinds of PP chains. As reported in our previous works,[47,53] the low molecular weight peak comes from PP chains with medium isotacticity (mi-PP), and the high molecular weight peak belongs to atactic PP (a-PP). The mi-PP chains have medium crystallinity and melting temperature around 140°C,[6,53] so most of them are insoluble in alkanes at room temperature. Appearance of some mi-PP chains in the C8-sol fractions should be attributed to their very low molecular weight ($\sim 1 \times 10^3$). By dividing the MWD curve into two parts at the lowest point between the two peaks, the average molecular weights of the two peaks were estimated respectively (see Table II).

The MWD curves of the C7-sol and C7-insol fractions were all monomodal (see the Supporting Information). As shown in Table II, molecular weight of the C7-sol fractions was rather low. This agrees with their easy dissolution in *n*-octane at room temperature when their chain length is shorter than a certain critical value. Molecular weight of the C7-insol fractions was the highest among the three fractions.

For the fractions of the PP/EPR alloys, MWD curve of the C8-sol fraction was also bimodal, but area of the peak located at about 1×10^3 was less than 2% of that of the main peak located at about 1×10^5 (see the Supporting Information). It has been proved that the low molecular weight peak is composed of mi-PP chains formed in the homopolymerization stage, while the main peak is a mixture of random ethylene–propylene copolymer (r-EP) formed in the copolymerization stage and a-PP formed in the homopolymerization stage.[6]

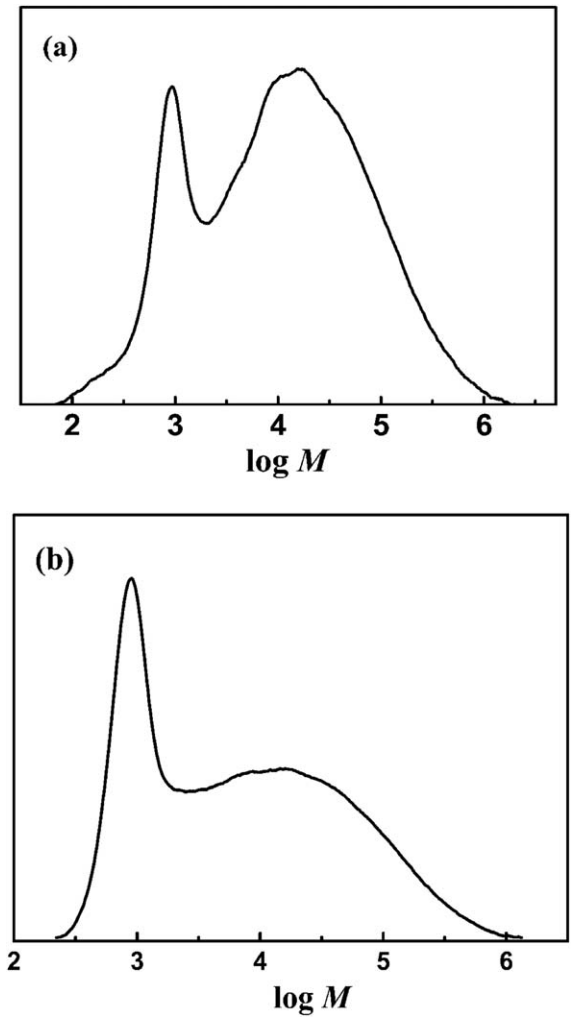

Figure 1. MWD curves of C8-sol fractions of PP: (**a**) PP-1; (**b**) PP-2.

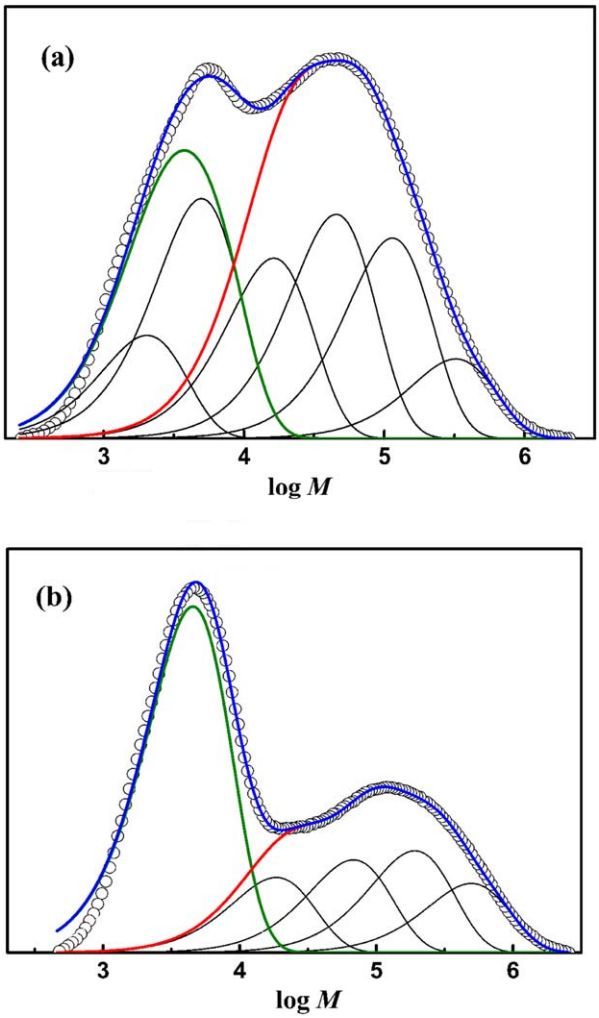

Figure 2. MWD curves of C7-sol fractions of PP/EPR alloys and their deconvolution into Flory components: (**a**) alloy-1; (**b**) alloy-2. (*Circles*: experimental data; *black lines*: Flory functions; *Green line*: sum of Flory components assigned to mi-PP; *Red line*: sum of Flory components assigned to s-EP; *Blue line*: sum of all the Flory components.). [Color figure can be viewed in the online issue, which is available at wileyonlinelibrary.com.]

MWD curve of the C7-sol fraction in the alloy was typical bimodal one, in which the two peaks had comparable areas (see Figure 2). The low molecular weight and high molecular weight parts of the bimodal MWD are composed of mi-PP and segmented ethylene-propylene copolymer (s-EP), respectively.[6] Based on short-chain-branch (SCB) frequency measured by GPC-IR instrument, Rungswang *et al.* have made a similar assignment of these two peaks in C7-sol fraction.[54] By deconvoluting the MWD curve into multiple Schulz–Flory "most-probable" distributions and adequately assigning the Flory components to the mi-PP or s-EP parts,[55] molecular weight of the two parts have been estimated and summarized in Table II. It can be seen that molecular weight of the s-EP chains are lower than that of the r-EP chains in the presence of CHMDMS (alloy-1), but the s-EP chains have higher molecular weight than the r-EP chains when DCPDMS was used as De.

MWD curve of the C7-insol fraction in the alloy was monomodal, similar to the C7-insol fraction of PP (see the Supporting Information). As disclosed in our previous works, this fraction is basically composed of highly isotactic PP (i-PP) chains.[26] Although the i-PP chains in the alloys have lower molecular weight than those in the propylene homopolymer (see Table II), considering that the alloys contain about 20% of copolymer chains which have longer main chain because of fewer short branches, the MFRs of the alloys are almost the same as the homopolymers (see Table I).

Chain Structures of HF-PP/EPR In-Reactor Alloys

Evaluating in depth the chain structure of high MFR polymers is an effect way to understand their physical properties, and in particular the melting and crystallization behaviors.[56] The chain structure of PP/EPR in-reactor alloys is more complicated than those of PP, because copolymer chains in the alloys may differ greatly in composition and comonomer sequence distributions. Among the two types of copolymer chains, the r-EP and the s-EP chains, s-EP with relatively long and crystallizable PE and PP segments play as compatibilizer between the PP matrix and the copolymer disperse phases.[4,5,26] Thus, the chain structure of s-EP was extremely important for understanding the relations between the chain structure and mechanical properties. However, as mentioned above, the C7-sol fraction is a mixture of s-EP and mi-PP, so the original sequence distribution data obtained from ^{13}C NMR spectrum of C7-sol fraction cannot represent the real chain structure of its s-EP chains for the overlapping of signals from PPP triads. By cutting the bimodal MWD curve into two parts at the lowest point between the two peaks, the weight ratio of mi-PP chains to s-EP chains can be estimated, and the comonomer sequence distribution of the s-EP part can be calculated.[6]

Table III. Original Sequence Distribution from ^{13}C NMR Analysis of C7-sol in HF-PP/EPR and Estimated Sequence Distribution of its s-EP part

	Original		s-EP	
	Alloy-1	Alloy-2	Alloy-1	Alloy-2
E	53.56	47.82	75.3	81.3
P	46.44	52.18	24.7	18.7
EE	49.85	42.70	67.9	73.2
EP	10.89	9.41	14.8	16.1
PP	39.26	47.89	17.3	10.6
EEE	46.15	39.32	62.9	67.4
EEP + PEE	7.41	6.76	10.1	11.6
PEP	0.00	1.74	0.00	3.0
EPE	3.75	2.59	5.1	4.4
PPE + EPP	6.86	3.40	9.3	5.8
PPP	35.83	46.19	12.6	7.7
$r_E' \cdot r_P'$[a]	-	-	21.4	12.0
n_E'[b]	-	-	10.2	10.1
n_P'[c]	-	-	3.3	2.3

[a] Product of reactivity ratios.
[b] Number average sequence length of ethylene unit.
[c] Number average sequence length of propylene unit.

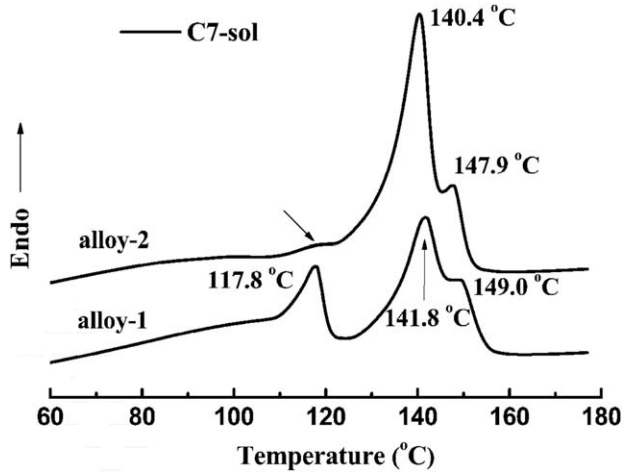

Figure 3. DSC melting traces of C7-sol fraction in HF-PP/EPR.

However, this method will introduce significant errors, because the two peaks in MWD curve were not symmetrical (see Figure 2). Based on satisfactory deconvolution of the MWD curve into several Flory components, we were able to assign the two Flory components of the lowest molecular weight as the mi-PP part in alloy-1, and assign the Flory component of the lowest molecular weight as the mi-PP part in alloy-2 (see Figure 2). Then the sequence distribution of the s-EP part was calculated by deducting the PPP triads of mi-PP from the original sequence distribution data (see the Supporting Information for calculation procedures). The assignments proposed by Randall on ^{13}C NMR spectra of ethylene-propylene copolymers[57] have been adopted for calculating the sequence distribution on the level of triads. Table III lists the original sequence distribution data and the estimated sequence distribution of the s-EP chains.

As seen in Table III, the sequence distribution of s-EP was much different from the original data obtained directly from the ^{13}C NMR results, because the contribution to PPP content by the mi-PP chains has been deducted. The propylene content of s-EP in alloy-1 is higher than that in alloy-2, meaning that using DCPDMA as De reduced insertion rate of propylene in this kind of active centers. The product of reactivity ratios

Table IV. Mechanical Properties of HF-PP and HF-PP/EPR Measured at 12°C

Samples	Flexural modulus E (MPa)	Flexural strength δ (MPa)	Izod impact strength (KJ/m^2)	Charpy impact strength (KJ/m^2)
PP-1	2235	56.1	1.27 ± 0.15	1.50 ± 0.13
PP-2	2541	58.6	1.70 ± 0.02	1.11 ± 0.03
Alloy-1	1439	35.5	6.16 ± 0.76	6.70 ± 1.02
Alloy-2	1804	43.8	5.35 ± 0.15	4.35 ± 0.21

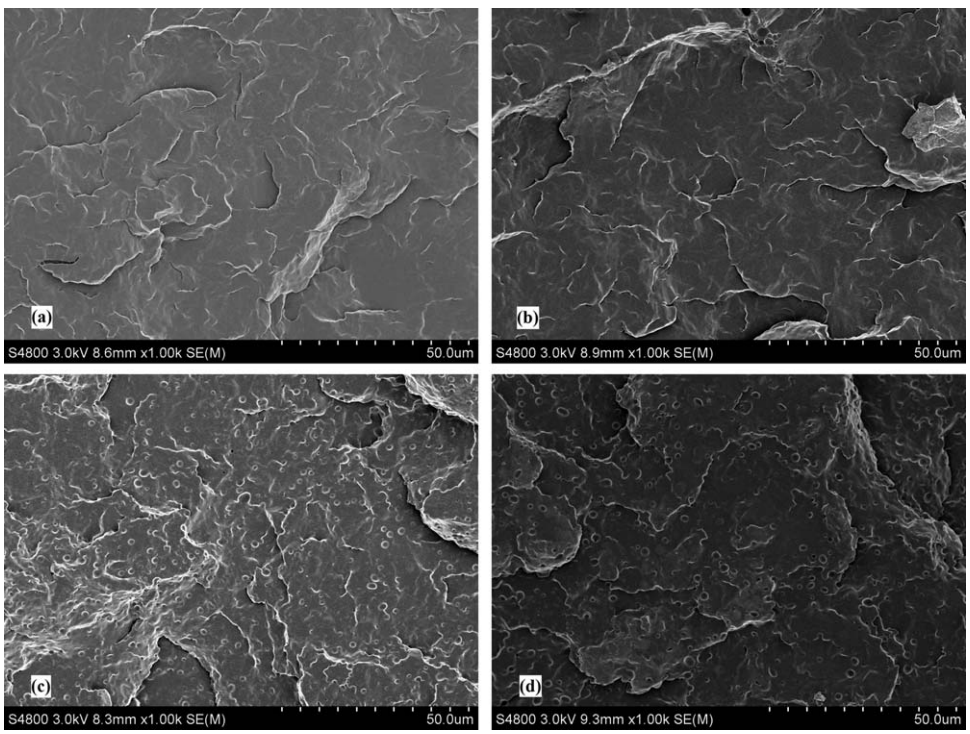

Figure 4. SEM photos of impact surfaces: (a) PP-1; (b) PP-2; (c) Alloy-1; and (d) Alloy-2.

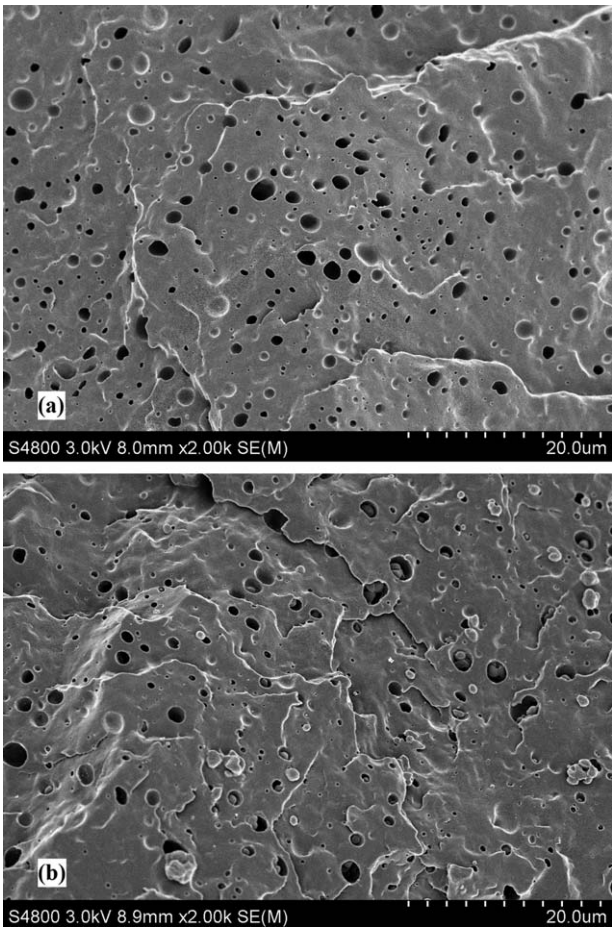

Figure 5. SEM micrographs for cryo-fractured surfaces etched by xylene of HF-PP/EPR in-reactor alloys: (a) Alloy-1; (b) Alloy-2.

$(r_E' \cdot r_P')$ can be used to qualitatively judge the type of sequence distribution. It shows that the $r_E' \cdot r_P'$ value of alloy-1 is 21.4, almost twice that of alloy-2, indicating higher blockiness of the s-EP chains formed in the presence of CHMDMS. In addition, the proportion of alternating triads PEP in alloy-1 is lower than that in alloy-2, which also shows a weaker blockiness in alloy-2.[58] The average sequence length of the ethylene unit (n_E') in these two alloys is almost the same, however, the average sequence length of the propylene unit (n_P') of alloy-1 is larger than that of alloy-2. It means that longer propylene segments are liable to be formed in the s-EP copolymer in alloy-1. Through above analysis, it seems the s-EP fraction in alloy-1 is more compatible with PP matrix than that in alloy-2.

The differences in chain structure of s-EP chains formed in the presence of CHMDMS and DCPDMS can be tentatively explained by the differences of the two De. As shown in Table III, the s-EP chains are rather blocky, meaning that they are composed of many long PE and PP segments connected sequentially. Such blocky copolymer chains might be formed by active centers that are oscillating between two states: a state with higher propylene incorporation rate that forms the PP segments, and a state with lower propylene incorporation rate that forms the PE segments. Such kind of oscillating active centers may exist when the De molecules cannot be adsorbed on the active sites firmly. Our previous work showed that De can reversibly adsorb on the active centers to change their catalytic behaviors.[47] In the ethylene–propylene copolymerization system, it can be expected that adsorption of De will lower the propylene incorporation rate, as the active centers will become more sterically hindered. When the De leaves the center through complexation with $AlEt_3$, propylene incorporation rate will recover to high level. Among the two De studied in this work, DCPDMS has a much larger equilibrium constant of adsorption on isospecific active centers than CHMDMS.[47] If the s-EP chains were produced by these isospecific active centers, because DCPDMS adsorbs on them more firmly than CHMDMS, the s-EP chains formed in the presence of DCPDMS will have shorter PP segments and lower blockiness.

Thermal analysis may provide useful information to understand the composition and chain structure of polymer. DSC melting traces of C7-sol fractions in the two HF-PP/EPR samples are shown in Figure 3. A strong melting peak at 140.4°C was observed in alloy-2, and a similar peak at 141.8°C existed in the curve of alloy-1. As mentioned above, C7-sol is a mixture of s-EP and mi-PP, and this melting peak can be assigned to mi-PP as its position and shape are almost the same as what observed in the DSC curve of C7-sol fraction of the PP homopolymer. An obvious melting peak at 117.8°C was observed in the curve of alloy-1 but hardly seen in alloy-2. This peak should come from crystallizable long PE segments. The melting point of PE is greatly affected by its lamellae thickness. Therefore, weak blockiness of copolymer chains in C7-sol of alloy-2 can be deduced, which is in agreement with the sequence distribution results.

Mechanical Properties of HF-PP/EPR In-Reactor Alloys

The mechanical properties of the HF-PP and HF-PP/EPR samples were measured and summarized in Table IV. Among the two HF-PP samples, the flexural modulus and flexural strength of PP-2 are both slightly higher. This may be attributed to its slightly higher isotacticity. Flexural modulus and flexural strength of the alloy synthesized in the presence of DCPDMS (alloy-2) was evidently higher than those of alloy-1. However, the impact properties of these two alloys are considered similar to each other due to the experimental error. Therefore, alloy-2 showed better toughness–stiffness balance than alloy-1.

Compared with HF-PP, the alloys exhibited lower flexural properties but higher impact strengths. It indicates that r-EP component as the toughening agent can effectively increase the toughness of HF-PP. For alloy-1, the flexural modulus and flexural strength are evidently lower but the impact strengths are higher than that of alloy-2. It has been found before that random copolymer makes the main contribution to toughening the materials.[26] If we use the ratio of Impact strength/r-EP content as an indicator of toughening efficiency of the copolymer phase, then the two alloy samples showed the same toughening efficiency (0.37 vs. 0.38, here the impact strength is the average value of Izod and Charpy impact strength). Thus, the higher

Table V. Statistical Results of the EPR Phases in the Alloys

Sample	Min. cavity area (μm^2)	Max. cavity area (μm^2)	Density[a] (Num/μm^2)	A_n[b] (μm^2)	PDI[c]
Alloy-1	7.4×10^{-3}	4.76	0.27	0.33	4.51
Alloy-2	7.4×10^{-3}	5.16	0.24	0.28	6.21

[a] Number of cavities per square micrometer counted in the SEM photo.
[b] Number average cavity area calculated according to the equation: $A_n = \Sigma(N_i A_i)/\Sigma N_i$, where N_i and A_i are number and area of cavities of a certain size, respectively.
[c] Polydispersity of the cavity area, PDI = A_a/A_n, where A_a is area average cavity area calculated according to the equation: $A_a = \Sigma(N_i A_i^2)/\Sigma(N_i A_i)$.

toughness of alloy-1 should be mainly attributed to its higher r-EP content than alloy-2.

On the other hand, the lower flexural modulus of the alloy than the PP homopolymer can also be attributed to the presence of copolymer phase, as the rather soft copolymer makes no contribution to stiffness. Because alloy-2 contains less copolymer than alloy-1, its flexural modulus is thus higher than the latter. However, higher stiffness of the i-PP part in alloy-2 may also contribute to its high flexural modulus.

Phase Morphology of HF-PP and HF-PP/EPR In-Reactor Alloys

Figure 4 displays the morphology of fractured surfaces of HF-PP and HF-PP/ERP. The surfaces of both HF-PP samples are smooth, with no wrinkles and coarse structures, which means typical features of brittle fracture. Nevertheless, as shown in the images of the alloys, many circular points, namely the copolymer phases, disperse in the PP matrix. They will absorb and transfer the stress, thus avoiding the matrix form yield deformation. On the fractured surfaces there are many coarse bulges, which is a mark of ductile fracture. Compared with alloy-1 prepared in the presence of CHMDMS, the surface of alloy-2 seems to be flatter, implying poor toughness.

In order to evaluate the phase structure, such as the number, size, and distribution of the dispersed phase domains, cryo-fractured surfaces of the alloys were observed by SEM. In Figure 5, biphasic structure can be clearly seen, and the dispersion phases are shown as tiny cavities left by EPR-rich domains etched by xylene. By comparison, it seems that quantity of cavities in alloy-1 is larger, and their size seems more uniform than Alloy-1. As the cavities range in different sizes and distribute unevenly, it is really difficult to compare the phase morphology of the two samples just by observation. With the help of an image analysis software, the number density and size distribution of the cavities were determined by counting and measuring the areas of cavities observed.[5] SEM pictures of ×2000 magnification were used in the image analysis.

As shown in Table V, the areas of cavities in alloy-2 range from 7.38×10^{-3} μm^2 to 5.16 μm^2, much wider than that in alloy-1. The average cavity size (A_n) in alloy-2 is smaller than that in alloy-1. Thus, it can be inferred that cavities in alloy-2 concentrated in small size range. Theoretically, disperse phases with smaller size in a certain range are beneficial to enhance the toughness. However, the cavity size distribution (A_a/A_n) of alloy-2 is much larger than that of alloy-1, which is unfavorable for the toughness improvement. In addition, the cavity density of alloy-1 is larger than that of alloy-2, which is in consistent with the fractionation result. Among the three factors that influence the effectiveness of toughening, alloy-1 synthesized in the presence of CHMDMS has larger cavity density and narrower cavity size distribution but a little larger cavity size than alloy-2 produced with DCPDMS. Therefore, the toughness of alloy-1 is higher than that of alloy-2. It can be concluded that an increase of EPR disperse phase can improve the impact strength of the alloy, but excessive amount is bound to weaken the rigidity. Elastomer content, size distribution of the disperse phase, nature of PP matrix, as well as phase compatibility will determine the final properties of the alloy. However, detailed relations between these factors and the polymer properties are to be clarified in future works.

CONCLUSIONS

In this work, high MFR PP and PP/EPR in-reactor alloys (MFR = 30 g/10 min) were synthesized with a commercial $MgCl_2$-supported Ziegler–Natta catalyst by adding relatively large amount hydrogen as chain transfer agent. Two kind of $R_1R_2Si(OMe)_2$ type external donors, CHMDMS and DCPDMS, were compared for polymerization activity, polymer chain structure and mechanical properties. To adjust the MFR to around 30 g/10 min, doubled amount of H_2 was needed when DCPDMS was used as the external donor. In synthesizing PP/EPR in-reactor alloys by sequential homopolymerization–copolymerization process, using CHMDMS as De leads to production of more ethylene-propylene copolymer, while the copolymer formed in the presence of DCPDMS has higher molecular weight. Using CHMDMS as the external donor, the formed segmented copolymer chains have higher blockiness than those formed in the presence of DCPDMS. The alloy prepared by DCPDMS exhibited higher flexural properties but lower impact strengths than that prepared by CHMDMS. Toughening efficiency of the rubber phase was nearly the same in the alloys prepared using CHMDMS and DCPDMS as De, but stiffness of the alloy can be improved by using DCPDMS.

ACKNOWLEDGMENTS

Support by the Major State Basic Research Programs (Grant 2011CB606001) and the Open Research Project of the State Key

Laboratory of Industrial Control Technology, Zhejiang University, China (No. ICT1528) is gratefully acknowledged.

REFERENCES

1. Zhang, X. F.; Xie, F.; Pen, Z. L.; Zhang, Y.; Zhang, Y. X.; Zhou, W. *Eur. Polym. J.* **2002**, *38*,
2. Tang, W. H.; Tang, J.; Yuan, H. L.; Jin, R. G. *J. Appl. Polym. Sci.* **2011**, *122*, 461.
3. Song, S. J.; Feng, J. C.; Wu, P. Y.; Yang, Y. L. *Macromolecules* **2009**, *42*, 7067.
4. Mehtarani, R.; Fu, Z. S.; Tu, S. T.; Fan, Z. Q.; Tian, Z.; Feng, L. F. *Ind. Eng. Chem. Res.* **2013**, *52*, 9775.
5. Mehtarani, R.; Fu, Z. S.; Fan, Z. Q.; Tu, S. T.; Feng, L. F. *Ind. Eng. Chem. Res.* **2013**, *52*, 13556.
6. Fu, Z. S.; Tu, S. T.; Fan, Z. Q. *Ind. Eng. Chem. Res.* **2013**, *52*, 5887.
7. Zhang, Y. Q.; Fan, Z. Q.; Feng, L. X. *J. Appl. Polym. Sci.* **2002**, *84*, 445.
8. Ryu, S. H.; Gogos, C. G.; Xanthos, M. *Polymer* **1991**, *32*, 2449.
9. Azizi, H.; Ghasemi, I. *Polym. Test.* **2004**, *23*, 137.
10. Jiang, Q.; Jia, H.; Wang, J.; Fang, E.; Jiang, J. *Iran. Polym. J.* **2012**, *21*, 201.
11. Tang, Y. Y.; Wang, J. Y.; Jia, H. B.; Ding, L. F.; Jiang, Q. *J. Appl. Polym. Sci.* **2013**, *130*, 2557.
12. Chen, Z. N.; Huang, F.; Li, Y. L.; Jia, X. L. *Chin. Synth. Resin Plast. (Chinese)* **2013**, *30*, 28.
13. Chadwick, J. C.; Miedema, A.; Sudmeijer, O. *Macromol. Chem. Phys.* **1994**, *195*, 167.
14. Kissin, Y. V.; Rishina, L. A. *J. Polym. Sci., Part A: Polym. Chem.* **2002**, *40*, 1353.
15. Kissin, Y. V.; Rishina, L. A.; Vizen, E. I. *J. Polym. Sci., Part A: Polym. Chem.* **2002**, *40*, 1899.
16. Mori, H.; Endo, M.; Terano, M. *J. Mol. Catal. A: Chem.* **1999**, *145*, 211.
17. Zhang, L. T.; Fan, L. N.; Fan, Z. Q.; Fu, Z. S. *e-Polymers* **2010**, 10, 167.
18. Alshaiban, A.; Soares, J. B. P. *Macromol. React. Eng.* **2013**, *7*, 135.
19. Azizi, H.; Ghasemi, I.; Karrabi, Q. *Polym. Test.* **2008**, *27*, 548.
20. Blackmon, K. P.; Barthel-rosa, L. P.; Malbari, S. A.; Rauscher, D. J.; Daumerie, M. M. U.S. Pat. 20,040,116,629, **2004**.
21. Naiki, M.; Matsumura, T.; Matsuda, M. *J. Appl. Polym. Sci.* **2002**, *83*, 46.
22. Grestenberger, G.; Potter, G. D.; Grein, C. *Express Polym. Lett.* **2014**, *8*, 282.
23. Bagheri-Kazemabad, S.; Fox, D.; Chen, Y.; Geever, L. M.; Khavandi, A.; Bagheri, R.; Higginbotham, C. L.; Zhang, H.; Chen, B. *Compos. Sci. Technol.* **2012**, *72*, 1697.
24. Liang, J. Z. *J. Polym. Environ.* **2012**, *20*, 872.
25. Liu, G. Y.; Qiu, G. X. *Polym. Bull.* **2013**, *70*, 849.
26. Fan, Z. Q.; Zhang, Y. Q.; Xu, J. T.; Wang, H. T.; Feng, L. X. *Polymer* **2001**, *42*, 5559.
27. Tu, S. T.; Fu, Z. S.; Fan, Z. Q. *J. Appl. Polym. Sci.* **2012**, *124*, 5154.
28. He, A. H.; Shi, Y. W.; Liu, G. Q.; Yao, W.; Huang, B. C. *Chin. J. Polym. Sci.* **2012**, *30*, 632.
29. Fan, Z. Q.; Deng, J.; Zuo, Y. M.; Fu, Z. S. *J. Appl. Polym. Sci.* **2006**, *102*, 2481.
30. Dong, Q.; Wang, X. F.; Fu, Z. S.; Xu, J. T.; Fan, Z. Q. *Polymer* **2007**, *48*, 5905.
31. Li, R.; Zhang, X.; Zhao, Y.; Hu, X.; Zhao, X.; Wang, D. *Polymer* **2009**, *50*, 5124.
32. Tian, Z.; Gu, X. P.; Wu, G. L.; Feng, L. F.; Fan, Z. Q.; Hu, G. H. *Ind. Eng. Chem. Res.* **2011**, *50*, 5992.
33. Tian, Z.; Gu, X. P.; Wu, G. L.; Feng, L. F.; Fan, Z. Q.; Hu, G. H. *Ind. Eng. Chem. Res.* **2012**, *51*, 2257.
34. Zhang, C. H.; Shangguan, Y. G.; Chen, R. F.; Zheng, Q. *J. Appl. Polym. Sci.* **2011**, *119*, 1560.
35. Xue, Y. H.; Fan, Y. D.; Bo, S. Q.; Ji, X. L. *Eur. Polym. J.* **2011**, *47*, 1646.
36. Gahleitner, M.; Tranninger, C.; Doshev, P. *J. Appl. Polym. Sci.* **2013**, *130*, 3028.
37. García, R. A.; Coto, B.; Expósito, M. T.; Suarez, I.; Fernández-Fernández, A.; Caveda, S. *Macromol. Res.* **2011**, *19*, 778.
38. Tian, Z.; Feng, L. F.; Fan, Z. Q.; Hu, G. H. *Ind. Eng. Chem. Res.* **2014**, *53*, 11345.
39. Zohuri, G. H.; Jamjah, R.; Ahmadjo, S. *J. Appl. Polym. Sci.* **2006**, *100*, 2220.
40. Alshaiban, A.; Soares, J. B. P. *Macromol. React. Eng.* **2014**, *8*, 723.
41. Amer, I.; van Reenen, A. *Macromol. Symp.* **2009**, *282*, 33.
42. Li, N.; Wang, X. F.; Dong, Q.; Fu, Z. S.; Fan, Z. Q. *Acta Polym. Sin. (Chinese)* **2006**, *4*, 632.
43. Chadwick, J. C.; Morini, G.; Balbontin, G.; Camurati, I.; Heere, J. J. R.; Mingozzi, I.; Testoni, F. *Macromol. Chem. Phys.* **2001**, *202*, 1995.
44. Wang, Q.; Murayama, N.; Liu, B. P.; Terano, M. *Macromol. Chem. Phys.* **2005**, *206*, 961.
45. Tu, S. T.; Lou, J. Q.; Fu, Z. S.; Fan, Z. Q. *e-Polymers* **2011**, *11*, 550.
46. Zhang, H. X.; Lee, Y. J.; Park, J. R.; Lee, D. H.; Yoon, K. B. *Macromol. Res.* **2011**, *19*, 622.
47. Shen, X. R.; Fu, Z. S.; Hu, J.; Wang, Q.; Fan, Z. Q. *J. Phys. Chem. C* **2013**, *117*, 15174.
48. Harding, G. W.; van Reenen, A. J. *Eur. Polym. J.* **2011**, *47*, 70.
49. Chang, H. F.; Li, H. Y.; Zheng, T.; Zhang, L. Y.; Yuan, W.; Li, L.; Huang, H.; Hu, Y. L. *J. Polym. Res.* **2013**, *20*, 207.
50. Priyanshu, B. V.; Sukhdeep, K.; Harshad, R. P.; Virendra, K. G. *J. Polym. Res.* **2011**, *18*, 235.
51. Kang, J.; Yang, F.; Wu, T.; Li, H. L.; Cao, Y.; Xiang, M. *Eur. Polym. J.* **2012**, *48*, 425.

52. Shen, X. R.; Fu, Z. S.; Fan, Z. Q. *Acta Polym. Sin. (Chinese)* **2013**, *12*, 1537.

53. Yu, Y.; Tu, S. T.; Fu, Z. S.; Xu, J. T.; Fan, Z. Q. *Petrochem. Technol. (Chinese)* **2011**, *40*, 673.

54. Rungswang, W.; Saendee, P.; Thitisuk, B.; Pathaweeisariyakul, T.; Cheevasrirungruang, W. *J. Appl. Polym. Sci.* **2013**, *128*, 3131.

55. Fan, Z. Q.; Feng, L. X.; Yang, S. L. *J. Polym. Sci., Part A: Polym. Chem.* **1996**, *34*, 3329.

56. Busico, V.; Cipullo, R. *Prog. Polym. Sci.* **2001**, *26*, 443.

57. Randall, J. C.; Hsieh, E. T. *Macromolecules* **1982**, *15*, 1584.

58. Agarwal, V.; van Erp, T. B.; Balzano, L.; Gahleitner, M.; Parkinson, M.; Govaert, L. E.; Litvinov, V.; Kentgens, A. P. M. *Polymer* **2014**, *55*, 896.